

# Simulation of depolarizing channel exploring maximally non separable spin-orbit mode

G.Tiago<sup>1,2</sup>, V.S. Lamego<sup>3</sup>, M.H.M Passos<sup>4</sup>, W. F. Balthazar<sup>1,5</sup>, and J. A. O. Huguenin<sup>1,2\*</sup>

<sup>1</sup> *Programa de Pós-graduação em Física - Instituto de Física - Universidade Federal Fluminense - Niterói - RJ - 24210-346, Brazil*

<sup>2</sup> *Instituto de Ciencias Exatas - Universidade Federal Fluminense - Volta Redonda - RJ - 27213-145 Brazil*

<sup>3</sup> *Instituto Federal de Educação, Ciência e Tecnologia do Paraná, Assis Chateaubrián - PR - 85935-000, Brazil*

*Volta Redonda - RJ - 27213-100 Brazil*

<sup>4</sup> *Centro Brasileiro de Pesquisas Físicas, Rua Dr. Xavier Sigaud, 150, Urca, Rio de Janeiro, 22290-180, RJ, Brazil*

<sup>5</sup> *Instituto Federal de Educação, Ciência e Tecnologia do Rio de Janeiro - IFRJ - Volta Redonda - RJ 27213-100, Brazil*

(Dated: February 17, 2026)

## Abstract

Depolarizing Channel is one of the most important noise model and constitute a reliable benchmark quantum information field. In this work we present a simple way to emulate depolarizing channel exploring a vector beam in a compact linear optical circuit. The evolution of different states are successfully reproduced. Our results are in excellent agreement compared with the results obtained by the spin-orbit Solovay-Kitaev decomposition for Depolarizing Channel, also presented here for the first time.

## I. INTRODUCTION

Quantum information processes are susceptible to decoherence, the main challenge for the realization of quantum information and quantum computation protocols [1]. Furthermore, it is very important for the study of the classical-quantum transition[2]. Modeling decoherence processes in quantum channels has a pivotal relevance once quantum networks require reliable channel for entanglement or quantum superposition distribution [3, 4].

Even Depolarizing Channel presents deleterious action on standard model of quantum Shannon theory, quantum communication network was achieved by combining two depolarizing channel to transmit classical information when they are combined in a quantum superposition [5]. Such as prediction of transmit information by means noise channel was verified experimentally [6, 7]. Perfect quantum communication can envisaged by using entanglement breaking channels [8]. Also quantum information can be transmitted in by using N completely depolarizing channels in a superposition of alternative causal orders [9]. Such as results reinforces the relevance of studies on depolarizing channels.

On the other hand, degree of freedom (DoF) of light has proven to be a very robust platform to explore quantum features. By using polarization and transverse mode DoF we can built the well-known spin-orbit modes [10] that presents the same mathematical structure of a two systems entangled state [11]. These Bell-like modes violate Bell's inequalities written for quantum entangled states [12, 13] and can be seen as a suitable test bed apparatus for quantum computation through proof of principle for quantum gates [14, 15]. In quantum communication, a BB84 protocol for quantum cryptography without shared reference

---

\* jose\_hugguenin@id.uff.br

frame was experimentally demonstrated [16]. The investigation of fundaments of quantum mechanics we can cite system-environment interaction [17], contextuality [18, 19], quantum thermodynamics [20], and transition from quantum-to-classical random walk [21]. By adding path degree of freedom, tripartite entangled state can be emulated [22]. Mixed states are also emulated by spin-orbit modes, as X-states [23, 24] that were used to experimentally measure Discord on an intense laser beam [25].

Degrees of freedom of light of intense laser beams were used to emulate quantum channel both in Markovian [26] and in Non-Markovian [27] regime. A very complete simulation of quantum channel with intense laser beam was the implementation of the Solovay-Kitaev (SK) decomposition by using transverse mode as a ancillary system [28]. However, depolarizing channel was not emulated.

In this paper we present a very compact linear optical circuit to emulate the dynamics of a single qubit in a depolarizing channel. We compare the results with the implementation of SK-decomposition with excellent agreement showing more robustness in the results. The paper is organized as follow. Section II presents theoretical background. Section III presents the experimental proposal. The results are presented in Section IV where also we compare with unprecedented results of emulation of Depolarizing channel with SK-decomposition. Concluding remarks are presented in Section V.

## II. THEORY

### A. Depolarizing Channel

The depolarizing channel is well known in quantum information theory. A qubit in a pure state described by the density matrix  $\rho$  has a probability  $\lambda$  to depolarize (become a mixed state) and  $(1 - \lambda)$  to remain the same. So, the map of this evolution is

$$\mathcal{E}(\rho) = \lambda \frac{\mathbb{I}}{2} + (1 - \lambda)\rho. \quad (1)$$

We can write the previous equation by using Pauli operators to write the map of Eq.1 in the sum-operator formalism [29]

$$\mathcal{E}(\rho) = \left(1 - \frac{3\lambda}{4}\right)\rho + \frac{\lambda}{4}(\sigma_x\rho\sigma_x + \sigma_y\rho\sigma_y + \sigma_z\rho\sigma_z). \quad (2)$$

We can find the most common Kraus operators for this channel if we consider a  $\lambda' = \frac{3\lambda}{4}$ , giving the map

$$\mathcal{E}(\rho) = (1 - \lambda')\rho + \frac{\lambda'}{3}(\sigma_x\rho\sigma_x + \sigma_y\rho\sigma_y + \sigma_z\rho\sigma_z), \quad (3)$$

where we see that the Kraus operators are

$$K_0 = \sqrt{1 - \lambda}I = \sqrt{1 - \lambda} \begin{pmatrix} 1 & 0 \\ 0 & 1 \end{pmatrix} \quad K_1 = \sqrt{\frac{\lambda}{3}}\sigma_x = \sqrt{\frac{\lambda}{3}} \begin{pmatrix} 0 & 1 \\ 1 & 0 \end{pmatrix} \quad (4)$$

$$K_2 = \sqrt{\frac{\lambda}{3}}\sigma_y = \sqrt{\frac{\lambda}{3}} \begin{pmatrix} 0 & -i \\ i & 0 \end{pmatrix} \quad K_3 = \sqrt{\frac{\lambda}{3}}\sigma_z = \sqrt{\frac{\lambda}{3}} \begin{pmatrix} 1 & 0 \\ 0 & -1 \end{pmatrix}. \quad (5)$$

With the Kraus operators and the fact that we can write  $\rho$  as

$$\rho = \frac{1}{2}(\mathbb{I} + \vec{r}\cdot\vec{\sigma}), \quad (6)$$

where  $\vec{r} = (r_x, r_y, r_z)$  is the Bloch vector and  $\vec{\sigma} = (\sigma_x, \sigma_y, \sigma_z)$  is a vector with the Pauli's matrices, we can study how the effect of the channel on the Bloch's sphere, and we can calculate the outcome

$$\sum_{a=0}^3 K_a \rho K_a^\dagger = \frac{1}{6} \begin{pmatrix} [3 + (3 - 4\lambda)r_z] & (3 - 4\lambda)(r_x - ir_y) \\ (3 - 4\lambda)(r_x + ir_y) & [3 - (3 - 4\lambda)r_z] \end{pmatrix} \quad (7)$$

To end, if we compare the Equations (7) and (3), we can see that the Bloch sphere contracts uniformly as a function of  $\lambda$ , as shown in Eq.(8) and in the Fig 1 as an example.

$$(r'_x, r'_y, r'_z) \rightarrow \left( \left(1 - \frac{4\lambda}{3}\right) r_x, \left(1 - \frac{4\lambda}{3}\right) r_y, \left(1 - \frac{4\lambda}{3}\right) r_z \right) \quad (8)$$

## B. Spin-Orbit modes

In order to emulate experimentally the interaction between a system and the environment, we will consider the degrees of freedom of light, the polarization and the Hermite-Gaussian transverse modes. It is known that polarization are related to the vector nature of the electromagnetic field, where we can write any polarization state considering the horizontal ( $\hat{e}_H$ ) and vertical ( $\hat{e}_V$ ) basis  $\{\hat{e}_H, \hat{e}_V\} \equiv \{H, V\}$ , and for the HG modes, we can have a basis with the first order modes considering the spatial function of the HG oriented along the

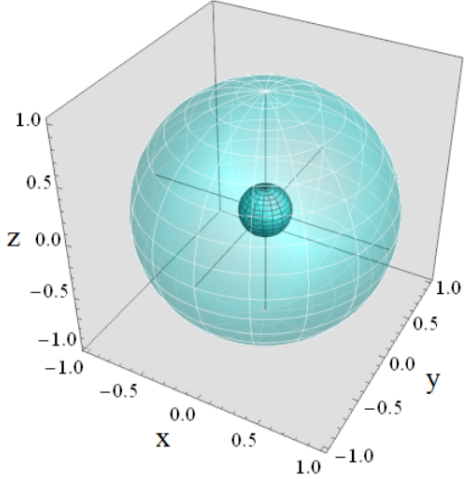


Figure 1. Contraction of Bloch sphere under depolarizing channel action.

horizontal ( $\psi_h$ ) and vertical ( $\psi_v$ ) directions  $\{\psi_h, \psi_v\} \equiv \{h, v\}$ . Therefore, this two degrees of freedom can be addressed independently, and a combined mode basis can be built from a tensor product of this two basis, and a beam with this two degrees are what we called Spin-Orbit (SO) modes. As discussed in Ref.[11], the quantization of the electromagnetic field in this basis lead to a bipartite system of internal degree of freedoms of single photon. Considering an intense laser beam can be described as a coherent state with a macroscopic number of photons, we use Dirac notation to describe DoF of the most general SO modes as [11]

$$|\Psi_{SO}\rangle = A_{Hh} |Hh\rangle + A_{Hv} |Hv\rangle + A_{Vh} |Vh\rangle + A_{Vv} |Vv\rangle. \quad (9)$$

where  $A_{ij}$  is the amplitude and  $\sum_{i,j} |A_{ij}|^2 = 1$ , with  $i = H, V$  and  $j = h, v$  being the polarization and transverse mode indexes. We can notice from Equation 9 that this modes can be separable and non-separable, i.e, we can factorized in product of transverse mode and polarization

$$|\Psi_{SO}\rangle = (A_h |h\rangle + A_v |v\rangle) \otimes (A_H |H\rangle + A_V |V\rangle), \quad (10)$$

where we used  $A_{ij} = A_i A_j$ . In this case we say the SO is separable. For any other situation the SO mode is called non-separable mode. The quantization of electromagnetic field in such as basis lead to entanglement between internal degree of freedom of light [11]. Note that Eq.9 present the same structure of a general bipartite system. Then, to characterize the spin-orbit separability with a definition similar to concurrence

$$C = 2|A_{Hh}A_{Vv} - A_{Hv}A_{Vh}|, \quad (11)$$

so, if  $C = 0$ , we have a separable mode, but if  $0 < C \leq 1$  is non-separable. The case  $C = 1$  indicates a maximally non-separable mode and can be written as

$$\begin{aligned} |\Phi_{\pm}\rangle &= \frac{|Hh\rangle \pm |Vv\rangle}{\sqrt{2}}, \\ |\Psi_{\pm}\rangle &= \frac{|Hv\rangle \pm |Vh\rangle}{\sqrt{2}}, \end{aligned} \quad (12)$$

that present the same mathematical structure of the maximally entangled Bell states. These maximally non-separable modes allows to study entanglement and quantum information with an intense laser beam and even with photons [10, 12, 13]. A complete study of the partial separability of these modes can be seen in ref. [30].

### C. Solvay-Kitaev decomposition

Few years ago, inspired by the Solovay-Kitaev theorem, it was demonstrated that any single-qubit CPTP channel  $\mathcal{E}$  can be decomposed into the convex combination as

$$\mathcal{E} = p\mathcal{E}_a^e + (1-p)\mathcal{E}_b^e, \quad (13)$$

where  $0 \leq p \leq 1$  and  $\mathcal{E}_i^e$ ,  $i = a, b$  are two quasi-extreme channels [31]. Such a decomposition can be implemented using one ancillary qubit, two CNOT gates, and four single-qubit operations, as shown in the logical circuit in Fig. 2 and described in Ref. [31]. The unitary operators  $U$  and  $U'$  belong to the SU(2) group and will assume different forms depending on the channel to be emulated with the SK-decomposition.

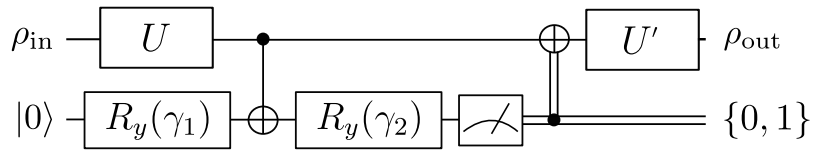


Figure 2. Logical circuit for implementing an arbitrary quantum channel  $\mathcal{E}$ , as defined in Eq. (13), acting on a single-qubit system. Note that the present circuit implements the channels  $\mathcal{E}_a^e$  and  $\mathcal{E}_b^e$  individually [31].

As detailed in Ref.[31],  $\mathcal{E}_i^e$  ( $i = a, b$ ) are represented in terms of modified Kraus operators

$$M_i = UK_iU'. \quad (14)$$

The map  $\mathcal{E} \equiv \mathcal{E}(\lambda, \alpha, \beta, \gamma_1, \gamma_2, p)$  where the parameters  $\lambda, \alpha, \beta$  are variables of the kraus operator, being  $\lambda$  associated to the evolution within the channel.  $\gamma_1$  and  $\gamma_2$  are angles related to rotation operations applied to the ancilla, while  $p$  is the weight associated with the convex combination of the quasi-extreme channels  $\mathcal{E}_{a,b}^e$ .

Our group implemented the SK-decomposition experimentally by using spin-orbit modes [32]. The system was codified in polarization DoF, while the ancilla was codified in the first-order Hermite-Gauss (HG) modes. For further details about the experimental implementation, Ref. [32] presents the optical circuit. In the referred experimental study, the operators  $R_y(\gamma)$  that acted in the HG mode are performed by a sequence of two Dove Prisms (DP), one horizontally oriented and the other rotated by  $\gamma/2$ . On the other hand,  $U$  and  $U'$  act on the polarization DoF (system) and are performed by a sequence of a Quarter wave plate, a Half wave-plate, and another Quarter wave-plate. Using such a combination of wave plates enables us to build a general unitary transformation on the SU(2) group. The  $U_{DP}$  operator is giving by

$$U_{DP} = QWP(0)HWP(\pi/2)QWP(-\pi/2). \quad (15)$$

All relations among the parameters of the SK-decomposition and the optical elements are established in detail in Ref.[32]. To conclude, the parameters required for the experimental realization of the depolarizing channel are listed in Table I.

$\lambda$	$\mathcal{E}_1^e$						$\mathcal{E}_2^e$						
	$\alpha$	$\beta$	$2\gamma_1$	$2\gamma_2$	$U$	$U'$	$\alpha$	$\beta$	$2\gamma_1$	$2\gamma_2$	$U$	$U'$	p
0	0	0	$\frac{\pi}{2}$	$-\frac{\pi}{2}$	none	none	$\frac{\pi}{4}$	$\frac{\pi}{4}$	$\frac{\pi}{2}$	0	$U_{DP}$	none	1
0.31	$\frac{\pi}{3}$	$\frac{\pi}{3}$	$\frac{\pi}{2}$	$\frac{\pi}{6}$	none	none	$\frac{\pi}{4}$	$\frac{\pi}{4}$	$\frac{\pi}{2}$	0	$U_{DP}$	none	0.76
0.5	$\frac{\pi}{6}$	$\frac{\pi}{6}$	$\frac{\pi}{2}$	$-\frac{\pi}{6}$	none	none	$\frac{\pi}{4}$	$\frac{\pi}{4}$	$\frac{\pi}{2}$	0	$U_{DP}$	none	0.66
0.75	$\frac{\pi}{4}$	$\frac{\pi}{4}$	$\frac{\pi}{2}$	0	none	none	$\frac{\pi}{4}$	$\frac{\pi}{4}$	$\frac{\pi}{2}$	0	$U_{DP}$	none	0.5
1	$\frac{\pi}{2}$	$\frac{\pi}{2}$	$\frac{\pi}{2}$	$\frac{\pi}{2}$	none	none	$\frac{\pi}{4}$	$\frac{\pi}{4}$	$\frac{\pi}{2}$	0	$U_{DP}$	none	0.33

Table I. Parameters to implement the Depolarizing channel in spin-orbit SK-decomposition.  $U_{DP}$  is the operator built to Depolarizing channel implementation.

## D. Quantum Coherence

Let us assume an arbitrary  $d$ -dimensional pure quantum state  $\rho$  described in a Hilbert space  $\mathcal{H}$ . The general form of an incoherent quantum state is written as

$$\delta = \sum_{k=0}^{d-1} p_k |k\rangle \langle k|, \quad (16)$$

where  $0 \leq p_k \leq 1$ , with  $\sum_k p_k = 1$ , and  $|k\rangle$  being an orthonormal reference basis. A proper measure of quantum coherence  $C(\rho)$  is defined as a nonnegative functional that vanishes on incoherent states and does not increase under incoherent completely positive and trace-preserving (ICPTP) operations [33]. One of the classes of coherence measurement is described in terms of the distance (or pseudo-distance)  $\mathcal{D}$  between the quantum state  $\rho$  and the closest incoherent state  $\delta_{min}$ , in such a way that

$$C(\rho) = \mathcal{D}(\rho, \delta_{min}). \quad (17)$$

Within the distance based quantum coherence measures, one of the most well-known is the coherence  $l_1$ -norm, which is defined as  $C(\rho) = \|\rho - \delta_{min}\|_{l_1}$ , where  $\|O\|_{l_1} = \sum_{k \neq k'} |\langle k| O |k'\rangle|$  denotes the  $l_1$ -norm of the operator  $O$  [33]. In this regard, the  $C_{l_1}$  takes the following form

$$C_{l_1}(\rho) = \sum_{k, k', k \neq k'} |\langle k| \rho |k'\rangle|, \quad (18)$$

In another way, if one assumes the density operator formalism for the case of one-qubit ( $d = 2$ ) state, where  $\rho = (I + \vec{r} \cdot \vec{\sigma})/2$ , with  $\vec{r} = (r_x, r_y, r_z)$  being the Bloch vector and  $\vec{\sigma} = (\sigma_x, \sigma_y, \sigma_z)$  representing the vector composed by Pauli matrices and  $I$  denoting the identity operator, the  $l_1$ -norm quantum coherence becomes

$$C_{l_1}(\rho) \equiv C_{l_1}(r_x, r_y) = \sqrt{r_x^2 + r_y^2}. \quad (19)$$

However, the  $l_1$ -norm quantum coherence is a basis-dependent concept, where even local unitary operations could change the quantum coherence of a given state. In this regard, a basis-free measure of quantum coherence can be defined if one performs a maximization over all *local* unitary transformations [34, 35] as follows

$$C_{\max}(\rho) = C(U_{\max} \rho U_{\max}^\dagger), \quad (20)$$

where  $U_{\max}$  describes a *local* unitary operation that maximizes  $C(\rho)$ . By assuming the operator  $U_{\max} = \sum_n |n_+\rangle \langle \psi_n|$ , where  $\{|\psi_n\rangle\}$  is the eigenstate of the quantum state  $\rho$  and  $\{|n_+\rangle\}$  is a mutually unbiased basis with respect to the incoherent basis  $\{|k\rangle\}$  [34], the maximum quantum coherence takes the form

$$C_{\max}(\rho) = \sum_{k,k'} |\langle k|\rho - I/d|k'\rangle|, \quad (21)$$

or, in terms of the Bloch sphere formalism,

$$C_{\max}(\rho) \equiv C_{\max}(r) = r. \quad (22)$$

In this work, beyond performing polarization state reconstruction via quantum tomography, we employ the  $l_1$ -norm ( $C_{l_1}$ ) and the maximum quantum coherence ( $C_{MAX}$ ) as figures of merit to quantify the effects of decoherence on a quantum state subjected to a depolarizing channel.

### III. PROPOSAL OF COMPACT CIRCUIT FOR DEPOLARIZING CHANNEL SIMULATION

The compact circuit that simulates the evolution of a quantum state under effect of a Depolarizing channel is presented in the Fig.3. In the same way as the SK-decomposition, our quantum state is described by a single qubit codified in the polarization DoF ( $|0\rangle \equiv |H\rangle$  and  $|1\rangle \equiv |V\rangle$ ) and the ancillary is codified in the transversal Gaussian ( $HG_{00} \equiv |G\rangle$ ) and Hermite-Gauss ( $HG_{10} \equiv |h\rangle$  and  $HG_{01} \equiv |v\rangle$ ) modes.

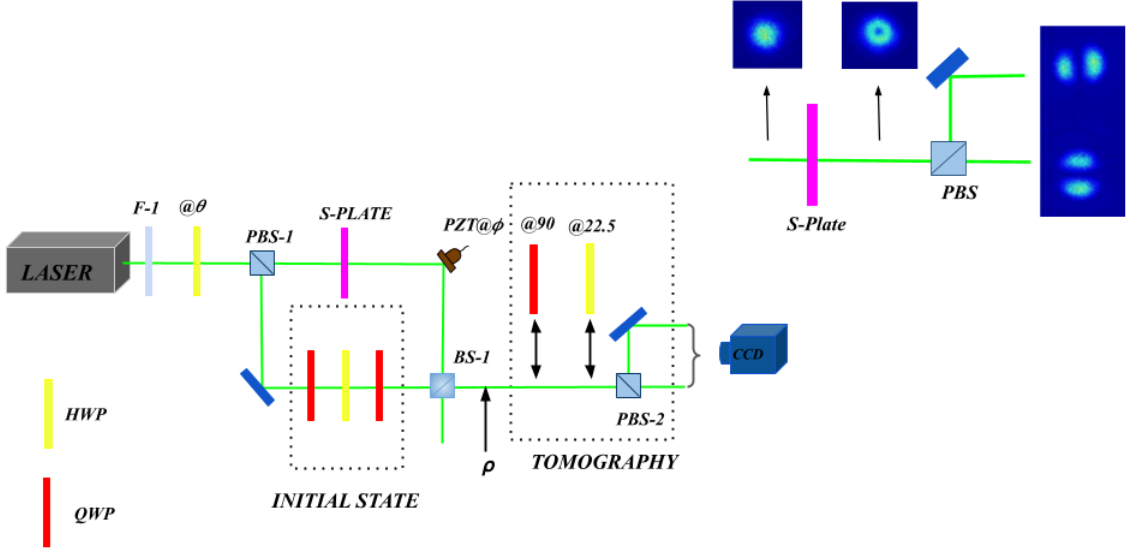


Figure 3. Experimental setup. S-plate prepares a maximally non-separable state, that presents maximally mixed polarization state by tracing transverse modes. The action of the S-plate in a Gaussian beam horizontally polarized is showed in the image at superior right part of the figure.

We begin with a vertically polarized laser beam (532 nm) passing through a filter (F-1) to attenuate its intensity. Therefore, we can write the initial state of the laser as

$$|\psi^0\rangle = |V\rangle \otimes |G\rangle = |VG\rangle, \quad (23)$$

afterwards, a Half Wave Plate (HWP) with an angle  $@\theta$  acts on the state  $|\psi^0\rangle$ , generating the state

$$|\psi^1\rangle = \{\sin(\theta) |H\rangle\} \otimes |G\rangle + \{-\cos(\theta) |V\rangle\} \otimes |G\rangle. \quad (24)$$

The next step is to position a polarized beam splitter (PBS-1), where the horizontal component is going to be transmitted, leaving the state to be only

$$|\psi^2\rangle = \{\sin(\theta) |H\rangle\} \otimes |G\rangle, \quad (25)$$

and the vertical is reflected

$$|\psi^3\rangle = \{-\cos(\theta) |V\rangle\} \otimes |G\rangle. \quad (26)$$

To prepare the state that will evolve under the channel, as well known, we can use a sequence of three wave plates in the arm of the reflected beam: a Quarter Wave Plate, a Half Wave

Plate, and a another Quarter Wave Plate. This set can perform arbitrary transformation in polarization degree of freedom, that corresponds to the preparation an arbitrary initial qubit. In this way, the we have the transformation  $|V\rangle \rightarrow \alpha|H\rangle + \beta|V\rangle$ , where  $\alpha$  and  $\beta$  are complex amplitudes and  $|\alpha|^2 + |\beta|^2 = 1$ , in other words, is a normalized state. The state in this arm becomes

$$|\psi^4\rangle = -\cos 2\theta(\alpha|H\rangle + \beta|V\rangle) \otimes |G\rangle. \quad (27)$$

The states that we are going to study are the vertical,  $|V\rangle$ , which implies  $\alpha = 0$  and  $\beta = 1$ , and diagonal,  $|+\rangle = \frac{|H\rangle + |V\rangle}{\sqrt{2}}$ , which implies  $\alpha = \beta = \frac{1}{\sqrt{2}}$ .

Now, we will focus on the transmitted beam, after the PBS-1, it passes through an S-wave plate, an optical element that can change the horizontal Gaussian beam into the maximal non-separable state  $\frac{1}{\sqrt{2}}(|Hh\rangle - |Vv\rangle)$

$$|\psi^5\rangle = \sin(2\theta) \frac{1}{\sqrt{2}}(|Hh\rangle - |Vv\rangle). \quad (28)$$

After the S-plate, the PZT gives a phase  $\phi$  between the paths. Moreover, to end the channel, the beams are put together in a beam splitter (BS-1), generating the state

$$|\psi^6\rangle = -\cos(2\theta)(\alpha|H\rangle + \beta|V\rangle) \otimes |G\rangle + e^{i\phi} \sin(2\theta) \frac{1}{\sqrt{2}}(|Hh\rangle - |Vv\rangle). \quad (29)$$

With our final state, we need to characterized it, this process is done by quantum state tomography, in this case, our tomography will be only in the polarization state, and the bases used where the computational base ( $\{|0\rangle, |1\rangle\}$ ), the diagonal/anti diagonal ( $\{|+\rangle, |-\rangle\}$ ) and the left/right circular ( $|L\rangle, |R\rangle$ ). This process allow us to only have the information of the polarization qubit, similar to a partial trace. Hence, if we take the density operator of Eq.(29)  $\rho = |\psi^6\rangle \langle \psi^6|$ , we can obtain the reduced density matrix of the polarization degree of freedom

$$\begin{aligned} \rho^{Pol} = & \cos^2(2\theta) \left( |\alpha|^2 |H\rangle \langle H| + \alpha\beta^* |H\rangle \langle V| + \beta\alpha^* |V\rangle \langle H| + |\beta|^2 |V\rangle \langle V| \right) + \\ & + \frac{\sin^2(2\theta)}{2} (|H\rangle \langle H| + |V\rangle \langle V|), \end{aligned} \quad (30)$$

which is analog to the expected final state after evolution in the Depolarizing channel. Note that for  $\theta = 0^\circ$ , which corresponds to  $\lambda = 0$ , we have the the initial state for polarization given by Eq.27. For  $\theta = 45^\circ$  ( $\lambda = 1$ ), we have the maximally mixed state for polarization as expected for  $t \rightarrow \infty$ . So if we consider the polarization space, we can simulate the depolarization of one qubit.

## IV. EXPERIMENTAL RESULTS

Lets us present the experimental results. In order to see the depolarization of an qubit, we simulate the evolution of two states:the computacional basis state  $\rho = |V\rangle\langle V|$  and the balanced superposition  $\rho = |+\rangle\langle +|$ . Such states able us to see the effect of the Depolarizing Channel.

We start by the unprecedeted results for Depolarizing Channel obtained by the spin-orbit implementation of the SK-decomposition. In the sequence, we show the results obtained by the proposed compact circuit.

### A. Results for the Solovay-Kitaev decomposition

Figure 4 present the density matrices of the polarization state for the evolution of the state  $|V\rangle$  (Vertical). In (a) we have de result for  $\lambda' = 0$ . As we can see, the matrix element  $HH$  should be null, but due to experimental error for the fidelity was compromised  $F = 71.86\%$ . This difficult for  $V$ -polarization can be explained by the complexity for the circuit of SK-decomposition, sequences of Dove Prisms that affect also the polarization, being more evident for initial state. As expected, the state evolution lead to partially mixed state (b) and (c), becoming totally mixed for  $\lambda' = 0.75$ , that corresponds to time sufficiently long ( $\lambda = 1$ ) in Fig. (d). For this state the Fidelity is  $F = 99.94\%$ .

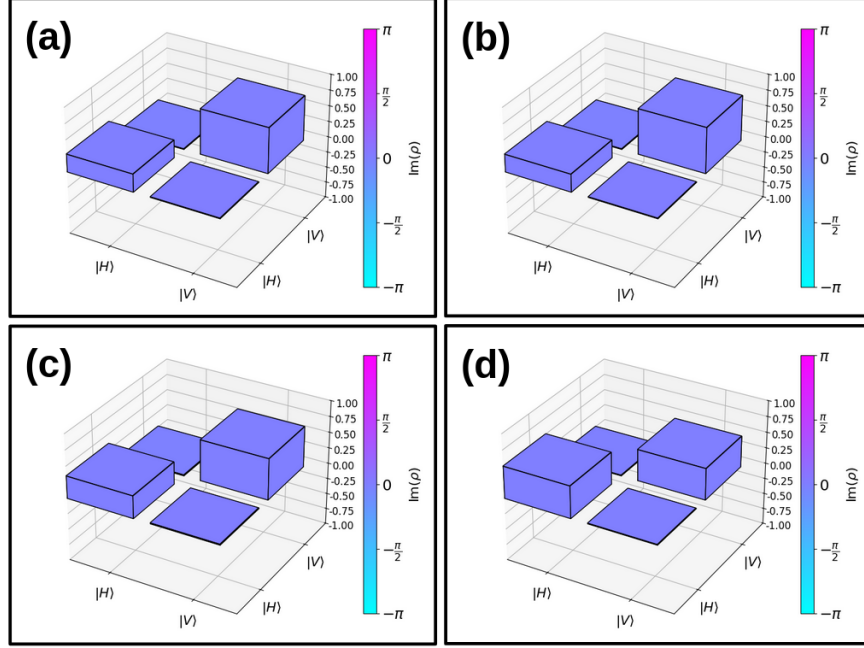


Figure 4. Density Matrices of the state  $\rho = |V\rangle\langle V|$  obtained from the Solovay-Kitaev decomposition. Where (a) is the probability  $\lambda' = 0$  of the state being depolarized, (b)  $\lambda' = 0.25$ , (c)  $\lambda' = 0.5$  and (d)  $\lambda' = 0.75$ .

Now, in Figure 5 we present the density matrices of the polarization state for the evolution of the state  $|+\rangle$  (Diagonal). Here, the initial state (a) for  $\lambda' = 0$  agreed more with the theoretical expectation after the propagation in the circuit ( $F = 94.78\%$ ). In the evolution, the maximally mixed state is achieved with Fidelity  $F = 99.82\%$  (d).

To analyze in a more deep way the accord with Quantum Theory, let us present the calculation of Coherence. Figure 6 present the results for  $l_1$ -norm Coherence (left) and Maximal Coherence (right). The experimental results for the state  $|V\rangle$  (vertical) is represented by gray squares and the for the state  $|+\rangle$  (Diagonal) by black circles

Vertical state does not present superposition and  $l_1$ -norm Coherence is expected to be null, as the Quantum Theory expectation showed by gray solid line. The experimental present a residual value due to experimental errors but remain constant during all process keeping the essence of the expected behavior. For the Diagonal state the theoretical expectation (black dashed line) is start to 1 and decreases to zero, with remarkable agreement of the experimental results.

For the maximal Coherence, as both vertical and Diagonal states are a pure states, the

expectation is  $C_{MAX}$  starts to 1 and vanishes linearly, as pointed by theoretical lines. The experimental results are in good agreement by exception of the case  $\lambda' = 0$ , that presents worst fidelity in the density matrix reconstruction.

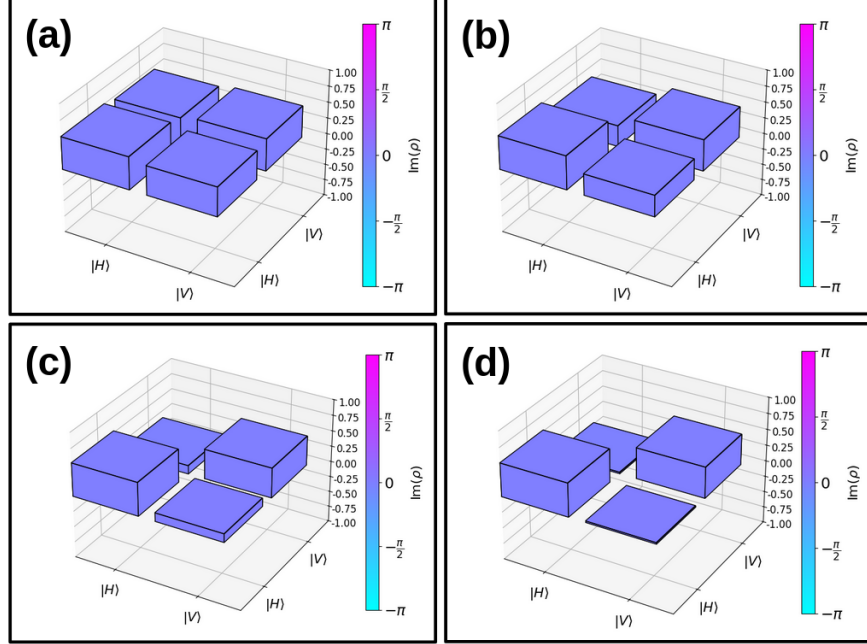


Figure 5. Density Matrices of the state  $\rho = |+\rangle\langle +|$  obtained from the Solovay-Kitaev decomposition. Where (a) is the probability  $\lambda' = 0$  of the state being depolarized, (b)  $\lambda' = 0.25$ , (c)  $\lambda' = 0.5$  and (d)  $\lambda' = 0.75$ .

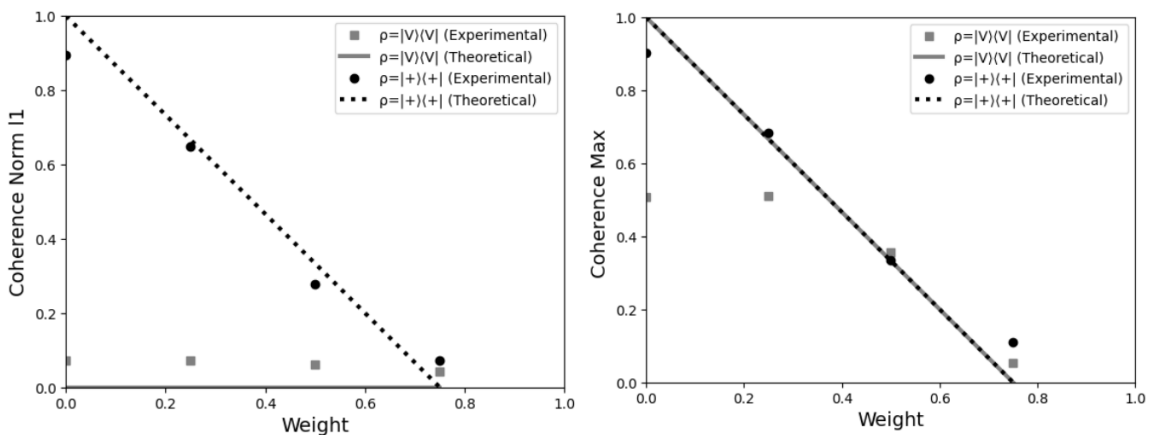


Figure 6. Maximal Coherence (left) and  $l_1$ Norm Coherence (right) for the simulation of Depolarizing Channel with Solovay-kitaev decomposition.

## B. Results for the proposed compact circuit

In this subsection we will present our experimental results from the proposed compact circuit. For the purpose of comparing our circuit with the Solovay-Kitaev, we simulate the same states, i.e,  $\rho = |V\rangle\langle V|$  and  $\rho = |+\rangle\langle +|$ . The first important aspect to mention is the facility to align and perform a complete measurement. Another important point to mention that here we emulate directly the weight  $\lambda$ .

Figures 7 and 8 present the false color output images for the polarization tomography for the states  $\rho = |V\rangle\langle V|$  and  $\rho = |+\rangle\langle +|$ , respectively. The group of images (I) corresponds to the experimental results and the group (II) the numerical simulation. Furthermore,  $I_i$  ( $i = H, V$ ) indicates the intensity output that is transmitted ( $I_H$ ) and reflected ( $I_V$ ) by the PBS<sub>2</sub> in the tomography process, and  $S_i$  ( $i=1,2,3$ ) indicates the calculated Stokes parameter.

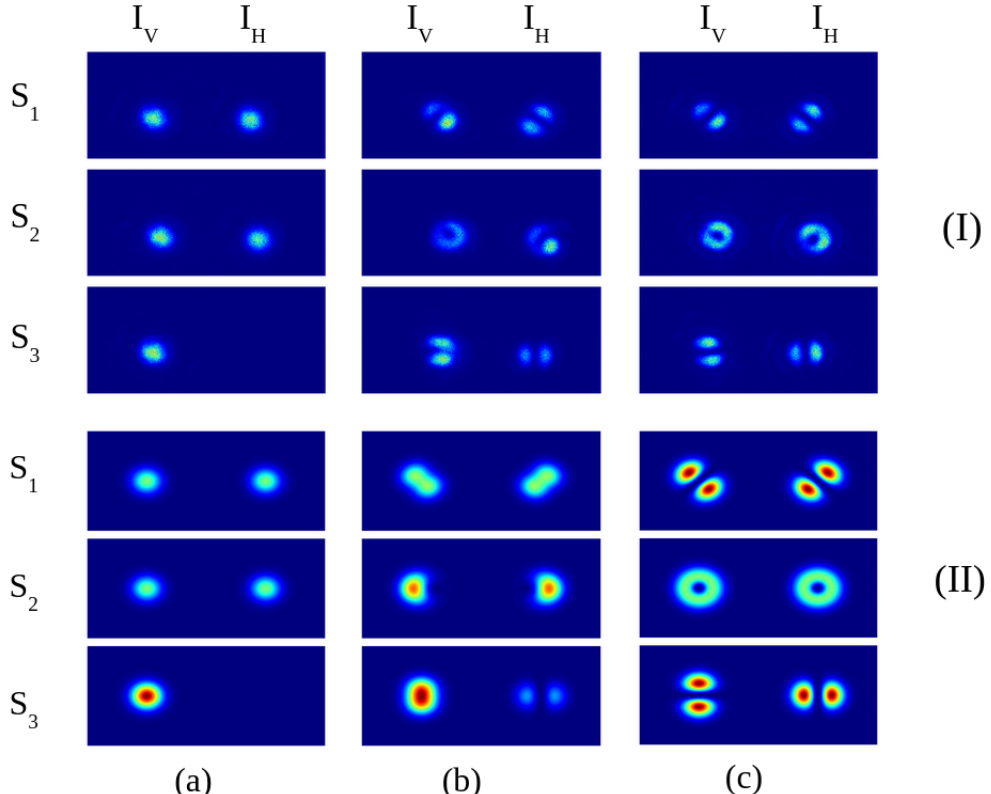


Figure 7. Tomography results for the state  $\rho = |V\rangle\langle V|$ , where (I) are the experimental results and (II) are the results from a computational simulation, with (a)  $\theta = 0$ , (b)  $\theta = 30$ , (c)  $\theta = 45$ .

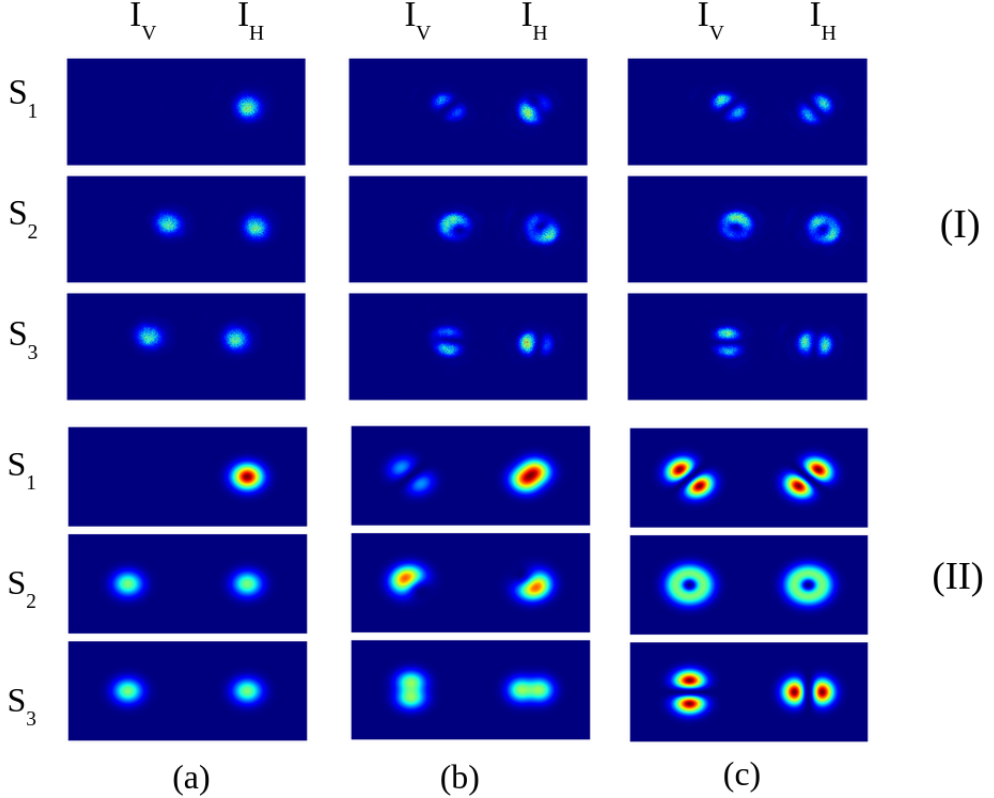


Figure 8. Tomography results for the state  $\rho = |+\rangle \langle +|$ , where (I) are the experimental results and (II) are the results from a computational simulation, with (a)  $\theta = 0$ , (b)  $\theta = 30$ , (c)  $\theta = 45$ .

In both cases we have a very good agreement between theory and experiment. Small difference in mode shape on intermediary evolution – Figures 7-b) and 8-b), due interference alignments does not affect the results, once to determine the polarization state density matrix we need only the normalized intensity projectes by PBS<sub>2</sub> to calculate the Stokes parameters and perform the state reconstitution.

Figure 9 show the density matrix for vertical state. A clear upgrade in the results is observed. For  $\lambda = 0$  the Fidelity was  $F = 100\%$  (a). The evolution arrived to the maximally mixed state (d) with  $F = 99.83\%$ . For the diagonal state  $\rho = |+\rangle \langle +|$ , Figure 10 bring the results also with excellent fidelities. For the final state, maximally mixed, we have Fidelity  $F = 99.91\%$ .

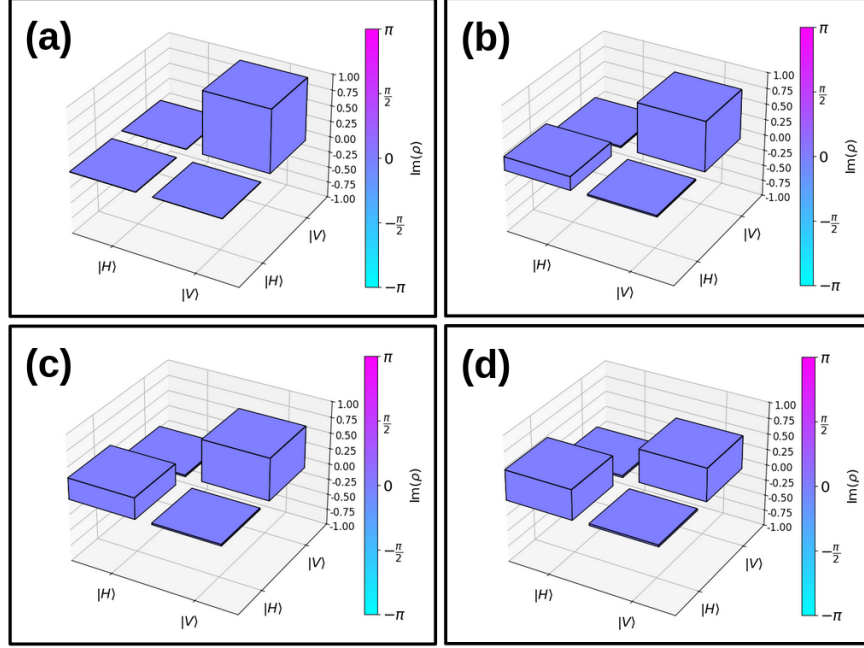


Figure 9. Density Matrices of the state  $\rho = |V\rangle \langle V|$  obtained from the compact circuit. Where (a) is the probability  $\lambda = 0$  of the state being depolarized, (b)  $\lambda = 0.40$ , (c)  $\lambda = 0.75$  and (d)  $\lambda = 1$ .

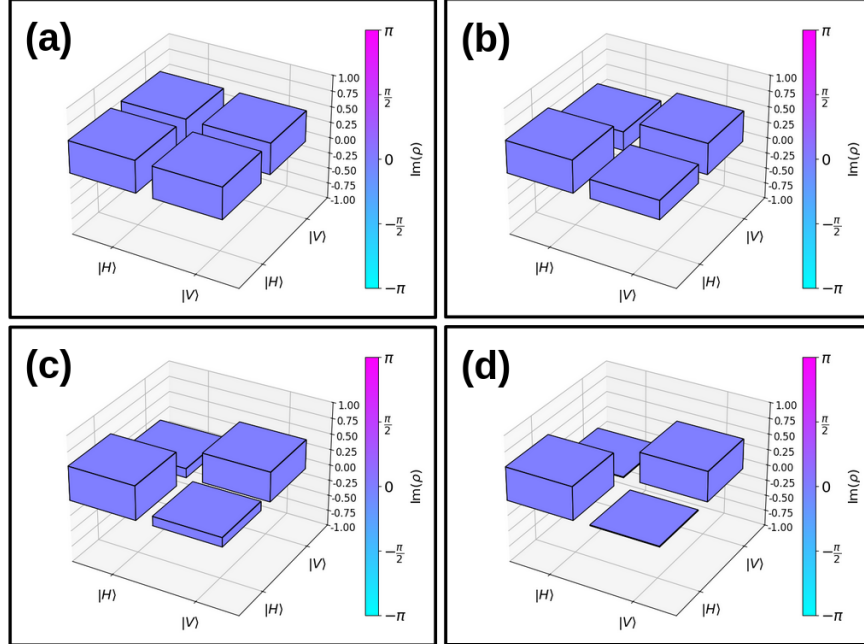


Figure 10. Density Matrices of the state  $\rho = |+\rangle \langle +|$  obtained from the compact circuit. Where (a) is the probability  $\lambda = 0$  of the state being depolarized, (b)  $\lambda = 0.40$ , (b)  $\lambda = 0.75$ , and (d)  $\lambda = 1$ .

The results for the Coherence are presented in Figure 11. As can be seen, we achieved

an excellent agreement with the expected by Quantum Theory. The accordance of  $C_{MAX}$  is superior to the one obtained by the SK-decomposition.

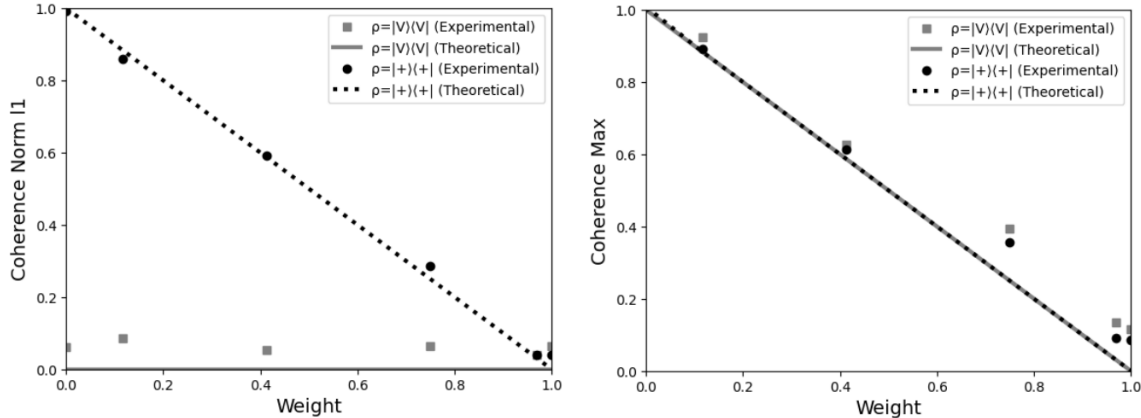


Figure 11. Maximal Coherence (left) and  $l_1$ Norm Coherence (right) for the simulation of Depolarizing Channel with the proposed compact circuit.

## V. CONCLUSIONS

In conclusion, we present the unprecedented simulation of the Depolarizing Channel with the spin-orbit modes implementation of Solovay-Kitaev decomposition. The results are in good agreement with the expected by Quantum Theory. The most important results of this work, however, is the proposal and experimental implementation of a compact linear optical circuit to emulate Depolarizing channel. The main idea is to increase the dimension of the Hilbert space of the system with an ancillary system and produce a state such that the partial trace in the ancillary produces the maximally mixed state of the system, and with it, we can perform a convex sum with the state of the system whose evolution we wish to study. In our case, our circuit explored the the maximally non-separable spin-orbit modes, that is analog of Bell state. By codifying the system in the polarization and use a S-plate we can perform exactly necessary transformations. Calculations of the unitary transformations of the circuit in the initial states show that the partial trace in the transverse mode is in excellent agreement with what is expected by quantum theory. The experimental results are in remarkable agreement with Quantum Theory. The results of compact circuit is much more robust of the ones pruduced by the circuit of Spin-Orbit Solovay-Kitaev decomposition. In addition, the simplicity of the circuit open an avenue to investigate superposition of

Depolarizing Channel.

**Acknowledgements** We would like to thank the financial support from the Brazilian funding agencies Conselho Nacional de Desenvolvimento Científico e Tecnológico (CNPq), Fundação Carlos Chagas Filho de Amparo à Pesquisa do Estado do Rio de Janeiro (FAPERJ), Coordenação de Aperfeiçoamento de Pessoal de Nível Superior (CAPES), National Institute for Science and Technology in Quantum Devices (INCT-QD / CNPq, Grant No. 408783/2024-9).

---

- [1] M. Schlosshauer, Quantum decoherence, *Physics Reports* **831**, 1 (2019).
- [2] W. H. Zurek, Decoherence, einselection, and the quantum origins of the classical, *Reviews of modern physics* **75**, 715 (2003).
- [3] D. Bruß, L. Faoro, C. Macchiavello, and G. M. Palma, Quantum entanglement and classical communication through a depolarizing channel, *Journal of Modern Optics* **47**, 325 (2000).
- [4] G. Riccardi, C. Antonelli, D. E. Jones, and M. Brodsky, Simultaneous decoherence and mode filtering in quantum channels: Theory and experiment, *Physical Review Applied* **15**, 014060 (2021).
- [5] D. Ebler, S. Salek, and G. Chiribella, Enhanced communication with the assistance of indefinite causal order, *Physical review letters* **120**, 120502 (2018).
- [6] K. Goswami, Y. Cao, G. A. Paz-Silva, J. Romero, and A. G. White, Increasing communication capacity via superposition of order, *Physical Review Research* **2**, 033292 (2020).
- [7] Y. Guo, X.-M. Hu, Z.-B. Hou, H. Cao, J.-M. Cui, B.-H. Liu, Y.-F. Huang, C.-F. Li, G.-C. Guo, and G. Chiribella, Experimental transmission of quantum information using a superposition of causal orders, *Physical review letters* **124**, 030502 (2020).
- [8] G. Chiribella, M. Banik, S. S. Bhattacharya, T. Guha, M. Alimuddin, A. Roy, S. Saha, S. Agrawal, and G. Kar, Indefinite causal order enables perfect quantum communication with zero capacity channels, *New Journal of Physics* **23**, 033039 (2021).
- [9] G. Chiribella, M. Wilson, and H. Chau, Quantum and classical data transmission through completely depolarizing channels in a superposition of cyclic orders, *Physical review letters* **127**, 190502 (2021).
- [10] C. E. R. Souza, J. A. O. Huguenin, P. Milman, and A. Z. Khoury, Topological phase

for spin-orbit transformations on a laser beam, *Physical Review Letters* **99**, 10.1103/physrevlett.99.160401 (2007).

- [11] L. J. Pereira, A. Z. Khoury, and K. Dechoum, Quantum and classical separability of spin-orbit laser modes, *Physical Review A* **90**, 053842 (2014).
- [12] C. V. S. Borges, M. Hor-Meyll, J. A. O. Huguenin, and A. Z. Khoury, Bell-like inequality for the spin-orbit separability of a laser beam, *Physical Review A* **82**, 10.1103/physreva.82.033833 (2010).
- [13] X.-F. Qian, B. Little, J. C. Howell, and J. H. Eberly, Shifting the quantum-classical boundary: theory and experiment for statistically classical optical fields, *Optica* **2**, 611 (2015).
- [14] C. E. R. Souza and A. Z. Khoury, A michelson controlled-not gate with a single-lens astigmatic mode converter, *Opt. Express* **18**, 9207 (2010).
- [15] W. F. Balthazar and J. A. O. Huguenin, Conditional operation using three degrees of freedom of a laser beam for application in quantum information, *J. Opt. Soc. Am. B* **33**, 1649 (2016).
- [16] C. E. R. Souza, C. V. S. Borges, A. Z. Khoury, J. A. O. Huguenin, L. Aolita, and S. P. Walborn, Quantum key distribution without a shared reference frame, *Phys. Rev. A* **77**, 032345 (2008).
- [17] M. H. M. Passos, W. F. Balthazar, A. Khoury, M. Hor-Meyll, L. Davidovich, and J. A. O. Huguenin, Experimental investigation of environment-induced entanglement using an all-optical setup, *Physical Review A* **97**, 022321 (2018).
- [18] T. Li, Q. Zeng, X. Song, and X. Zhang, Experimental contextuality in classical light, *Scientific* **7**, 1 (2017).
- [19] M. H. M. Passos, W. F. Balthazar, J. A. de Barros, C. E. R. Souza, A. Z. Khoury, and J. A. O. Huguenin, Classical analog of quantum contextuality in spin-orbit laser modes, *Phys. Rev. A* **98**, 062116 (2018).
- [20] M. H. M. Passos, A. C. Santos, M. S. Sarandy, and J. A. O. Huguenin, Optical simulation of a quantum thermal machine, *Phys. Rev. A* **100**, 022113 (2019).
- [21] V. Lamego, G. Cruz, D. Lima, S. Al-Kuwari, and J. Huguenin, Transition from quantum-to-classical random? pag\break?; walk distributions with spin-orbit modes, *Optics Letters* **49**, 6904 (2024).
- [22] W. F. Balthazar, C. E. R. Souza, D. P. Caetano, E. F. Galvão, J. A. O. Huguenin, and A. Z. Khoury, Tripartite nonseparability in classical optics, *Opt. Lett.* **41**, 5797 (2016).
- [23] W. F. Balthazar, D. G. Braga, V. S. Lamego, M. H. M. Passos, and J. A. O. Huguenin,

Spin-orbit  $x$  states, Phys. Rev. A **103**, 022411 (2021).

[24] D. G. Braga, I. Fonseca, W. F. Balthazar, M. S. Sarandy, and J. A. O. Huguenin, Spin-orbit maximally discordant mixed states, Phys. Rev. A **106**, 062403 (2022).

[25] V. S. Lamego, D. G. Braga, W. F. Balthazar, and J. A. O. Huguenin, Experimental investigation of quantum discord in spin-orbit  $x$  states, Phys. Rev. A **110**, 032601 (2024).

[26] P. Obando, M. Passos, F. Paula, and J. A. O. Huguenin, Simulating markovian quantum decoherence processes through an all-optical setup, Quantum Information Processing **19**, 7 (2020).

[27] M. Passos, P. C. Obando, W. Balthazar, F. Paula, J. Huguenin, and M. Sarandy, Non-markovianity through quantum coherence in an all-optical setup, Optics letters **44**, 2478 (2019).

[28] M. H. M. Passos, A. d. O. Junior, M. C. de Oliveira, A. Z. Khoury, and J. A. O. Huguenin, Spin-orbit implementation of the solovay-kitaev decomposition of single-qubit channels, Phys. Rev. A **102**, 062601 (2020).

[29] M. A. Nielsen and I. L. Chuang, *Quantum Computation and Quantum Information* (Cambridge University Press, 2000).

[30] V. Lamego, D. Braga, L. Oliveira, W. Balthazar, and J. Huguenin, Partial nonseparability of spin-orbit modes, Journal of Optics **25**, 034001 (2023).

[31] D.-S. Wang, D. W. Berry, M. C. de Oliveira, and B. C. Sanders, Solovay-kitaev decomposition strategy for single-qubit channels, Phys. Rev. Lett. **111**, 130504 (2013).

[32] M. Passos, A. d. O. Junior, M. de Oliveira, A. Khoury, and J. Huguenin, Spin-orbit implementation of the solovay-kitaev decomposition of single-qubit channels, Physical Review A **102**, 062601 (2020).

[33] T. Baumgratz, M. Cramer, and M. B. Plenio, Quantifying coherence, Phys. Rev. Lett. **113**, 140401 (2014).

[34] C.-s. Yu, S.-r. Yang, and B.-q. Guo, Total quantum coherence and its applications, Quantum Inf. Process. **15**, 3773 (2016).

[35] A. Streltsov, H. Kampermann, S. Wölk, M. Gessner, and D. Bruß, Maximal coherence and the resource theory of purity, New J. Phys. **20**, 053058 (2018).